Appl. Math. J. Chinese Univ.
2020, 35(3): 359-378

An efficient cubic trigonometric B-spline collocation scheme for the time-fractional telegraph equation

Muhammad Yaseen   Muhammad Abbas*

Abstract. In this paper, a proficient numerical technique for the time-fractional telegraph equation (TFTE) is proposed. The chief aim of this paper is to utilize a relatively new type of B-spline called the cubic trigonometric B-spline for the proposed scheme. This technique is based on finite difference formulation for the Caputo time-fractional derivative and cubic trigonometric B-splines based technique for the derivatives in space. A stability analysis of the scheme is presented to confirm that the errors do not amplify. A convergence analysis is also presented. Computational experiments are carried out in addition to verify the theoretical analysis. Numerical results are contrasted with a few present techniques and it is concluded that the presented scheme is progressively right and more compelling.

§1 Introduction

In recent years, the tools of fractional calculus have been effectively used to portray numerous physical phenomena in science and engineering [12, 17, 23]. Recently, there have been reporting of many applications typically expressed by fractional partial differential equations (FPDEs). The importance of FPDEs lies in the way that the solutions offered by FPDEs have descriptions that well approximate the chemical, physical and biological phenomena than their integer order counterparts. Accordingly, FPDEs have accomplished special status among researchers and engineers.

A number of phenomenon such as propagation of electric signals [14], transport of neutron in a nuclear reactor [28] and random walks [5] are described by a class of hyperbolic partial differential equations called the fractional telegraph equations [8]. The general form of the TFTE is given by

$$\frac{\partial^{\gamma} u(x,t)}{\partial t^{\gamma}} + \gamma_1 \frac{\partial^{\gamma-1} u(x,t)}{\partial t^{\gamma-1}} + \gamma_2 u(x,t) = \gamma_3 \frac{\partial^2 u(x,t)}{\partial x^2} + f(x,t), \tag{1}$$

Received: 2019-08-17.   Revised: 2020-03-20.
MR Subject Classification: 65M70, 65Z05, 65D05, 65D07, 35B35.
Keywords: Time-fractional telegraph equation, finite difference method, Cubic trigonometric B-splines collocation method, Stability, Convergence.
Digital Object Identifier(DOI): https://doi.org/10.1007/s11766-020-3883-y.
*Corresponding author.

with initial conditions

$$u(x,0) = \phi_1(x), u_t(x,0) = \phi_2(x), \qquad a \leq x \leq b, \tag{2}$$

and the boundary conditions

$$u(a,t) = \psi_1(t), u(b,t) = \psi_2(t), \qquad 0 \leq t \leq T, \tag{3}$$

where $1 < \gamma < 2$, $a, b, \phi_1(x), \phi_2(x), \psi_1(t)$ and $\psi_2(t)$ are given and $\frac{\partial^\gamma}{\partial t^\gamma}u(x,t)$ represents the Caputo fractional derivative of order γ given by [2, 4, 12, 15–17, 23, 31]

$$\frac{\partial^\gamma}{\partial t^\gamma}u(x,t) = \begin{cases} \frac{1}{\Gamma(n-\gamma)}\int\limits_0^t \frac{\partial^n u(x,s)}{\partial s^n}(t-s)^{n-\gamma-1}ds, & n-1<\gamma<n \\ \frac{\partial^n u(x,s)}{\partial s^n}, & \gamma = n. \end{cases} \tag{4}$$

Moreover, $\gamma_1, \gamma_2, \gamma_3$ are given positive constants. Note that in case of $\gamma = 2$, equation (1) corresponds to the classical second-order telegraph equation.

Various numerical and analytical methods are accessible in literature for the TFTE. Tasbozan and Esen [27] utilized a B-spline Galerkin method for the numerical solutions fractional telegraph equation. Hosseini *et al.* [10] made use of radial basis functions to obtain the numerical solution of TFTE. Akram *et al.* [2] solved the TFTE using extended cubic B-spline collocation method. Sweilam *et al.* [25] used Sinc-Legendre collocation procedure to find the approximate solution of time-fractional-order telegraph equation. A classic work of Orsinger and Zhao [22] regarding the space-fractional telegraph equation and the related fractional telegraph process appeared in 2003. S. Momani [20] obtained analytic and approximate solutions of the space and TFTE. Chen *et al.* [7] utilized the method of separating variables to obtain analytical solutions for the TFTE. Wei *et al.* [29] presented a fully discrete local discontinuous Galerkin method for solving the fractional telegraph equation. Wang *et al.* [30] used a reproducing kernel for solving a class of TFTE with initial value conditions. Hashemi and Baleanu [9]]utilized a geometric approach and the method of lines to obtain a numerical approximation of higher-order TFTE. Jiang and Lin [13] obtained the exact solution of the TFTE in the reproducing kernel space. In [18], Kumar presented new analytical modeling for fractional-telegraph equation via Laplace transform. Mollahasani *et al.* [21] developed a new technique based on hybrid functions for the numerical treatment of telegraph equations of fractional order. Hariharan *et al.* [11] utilized a wavelet method for a class of space and TFTE. Analytical solutions of space and TFTE were obtained by Yildirim [34] by using He's homotopy perturbation method.

The important motivation behind this paper is to present a numerical scheme for the TFTE that is computationally proficient and provides better results than some current numerical procedures [10, 25, 27]. To authors learning this paper is first endeavor towards finding the numerical solution of TFTE using cubic trigonometric B-splines. A detailed stability analysis of the scheme is presented to attest that errors do not amplify. A convergence analysis is also presented. Numerical experiments are performed to additionally set the precision and legitimacy of the procedure.

The remainder of the paper is composed as follows. In section 2, the numerical scheme primarily based on cubic trigonometric B-splines is derived in detail. Section 3 discusses the stability analysis. Section 4 talks about the convergence analysis. Section 5 demonstrates a comparison of our numerical results with those of [10, 25, 27]. Section 6 summarizes the conclusions of this study.

§2 The Derivation of the Scheme

For given positive integers M and N, let $\tau = \frac{T}{N}$ be the temporal and $h = \frac{b-a}{M}$ the spatial step sizes respectively. Following the usual notations, set $t_n = n\tau$ $(0 \leq n \leq N)$, $x_j = jh$, $(0 \leq j \leq M)$. Let u_j^n be approximation to exact solution at the point (x_j, t_n). The solution domain $a \leq x \leq b$ is uniformly partitioned by knots x_i into M subintervals $[x_j, x_{j+1}]$ of equal length h, $j = 0, 1, 2, ..., M-1$, where $a = x_0 < x_1 < ... < x_{n-1} < x_M = b$. Our scheme for solving (1) requires approximate solution $U(x,t)$ to the exact solution $u(x,t)$ in the following form [6, 24]

$$U(x,t) = \sum_{j=-1}^{N-1} c_j(t) TB_j^4(x), \tag{5}$$

where $c_j(t)$ are unknowns to be determined and $TB_j^4(x)$ [1] are twice differentiable cubic trigonometric basis functions given by

$$TB_j^4(x) = \frac{1}{w}\begin{cases} p^3(x_j) & x \in [x_j, x_{j+1}] \\ p(x_j)(p(x_j)q(x_{j+2}) + q(x_{j+3})p(x_{j+1})) + q(x_{j+4})p^2(x_{j+1}), & x \in [x_{j+1}, x_{j+2}] \\ q(x_{j+4})(p(x_{j+1})q(x_{j+3}) + q(x_{j+4})p(x_{j+2})) + p(x_j)q^2(x_{j+3}), & x \in [x_{j+2}, x_{j+3}] \\ q^3(x_{j+4}), & x \in [x_{j+3}, x_{j+4}] \end{cases} \tag{6}$$

where,$p(x_j) = \sin(\frac{x-x_j}{2})$, $q(x_j) = \sin(\frac{x_j-x}{2})$, $w = \sin(\frac{h}{2})\sin(h)\sin(\frac{3h}{2})$. Due to local support property of the cubic trigonometric B-splines only $TB_{j-1}^4(x), TB_j^4(x)$ and $TB_{j+1}^4(x)$ are survived so that the approximation u_j^n at the grid point (x_j, t_n) at n^{th} time level is given as [3, 19, 31, 33]:

$$u(x_j, t_n) = u_j^n = \sum_{j=i-1}^{i+1} c_j^n(t) TB_j^4(x). \tag{7}$$

The time dependent unknowns $c_j^n(t)$ are to be determined by making use of the initial and boundary conditions, and the collocation conditions on $TB_j^4(x)$. As a result the approximations u_j^n and its necessary derivatives are given as:

$$u_j^n = a_1 c_{j-1}^n + a_2 c_j^n + a_1 c_{j+1}^n, (u_j^n)_x = -a_3 c_{j-1}^n + a_3 c_{j+1}^n, (u_j^n)_{xx} = a_4 c_{j-1}^n + a_5 c_j^n + a_4 c_{j+1}^n, \tag{8}$$

where,
$a_1 = \csc(h)\csc(\frac{3h}{2})\sin^2(\frac{h}{2})$, $a_2 = \frac{2}{1+2\cos(h)}$,$a_3 = \frac{3}{4}\csc(\frac{3h}{2})$,
$a_4 = \frac{3+9\cos(h)}{4\cos(\frac{h}{2})-4\cos(\frac{5h}{2})}$,$a_5 = -\frac{3\cot^2(\frac{h}{2})}{2+4\cos(h)}$.
Following [10], the fractional derivatives $\frac{\partial^\gamma}{\partial t^\gamma}u(x,t)$ and $\frac{\partial^{\gamma-1}}{\partial t^{\gamma-1}}u(x,t)$ are discrtetized as:

$$\frac{\partial^\gamma}{\partial t^\gamma}u(x, t_{n+1}) = \alpha_0 \sum_{l=0}^{n} b_l(u(x, t_{n+1-l}) - 2u(x, t_{n-l}) + u(x, t_{n-1-l})) + r_1^{n+1}$$

$$= \alpha_0 \sum_{l=0}^{n} b_l (u^{n+1-l} - 2u^{n-l} + u^{n-1-l}) + r_1^{n+1}, 1 < \gamma < 2 \tag{9}$$

and

$$\frac{\partial^{\gamma-1}}{\partial t^{\gamma-1}} u(x, t_{n+1}) = \alpha_0 \tau \sum_{l=0}^{n} b_l (u(x, t_{n+1-l}) - u(x, t_{n-l})) + r_2^{n+1}$$
$$= \alpha_0 \tau \sum_{l=0}^{n} b_l (u^{n+1-l} - u^{n-l}) + r_2^{n+1}, 0 < \gamma - 1 < 1, \tag{10}$$

where $\alpha_0 = \frac{1}{\tau^\gamma \Gamma[3-\gamma]}$, $b_l = (l+1)^{2-\gamma} - l^{2-\gamma}$, r_1^{n+1} and r_2^{n+1} are truncation errors. It is straight forward to confirm that

- $b_l > 0, \quad l = 0, 1, \cdots, n.$
- $1 = b_0 > b_1 > b_2 > \cdots > b_n$ and $b_n \to 0$ as $n \to \infty$.
- $\sum_{l=0}^{n-1} (b_l - b_{l+1}) + b_n = 1.$

It is shown in [10] that $r_1^{n+1} \le \Lambda \tau$ and $r_2^{n+1} \le \Lambda \tau^{3-\gamma}$, where Λ is constant dependent on u, γ and T. To obtain temporal discretization, we substitute (9) and (10) into (1) to get

$$\alpha_0 \sum_{l=0}^{n} b_l (u^{n+1-l} - 2u^{n-l} + u^{n-1-l}) + \gamma_1 \tau \alpha_0 \sum_{l=0}^{n} b_l (u^{n+1-l} - u^{n-l}) + \gamma_2 u^{n+1} - \gamma_3 \frac{\partial^2 u^{n+1}}{\partial x^2}$$
$$= f^{n+1}. \tag{11}$$

It is observed that the term u^{-1} will appear when $n = 0$ or $l = n$. Using the central forward difference formula, we utilize the given initial condition to obtain

$$u_t^0 = \frac{u^1 - u^{-1}}{2\tau}. \tag{12}$$

From (12), we observe that $u^{-1} = u^1 - 2\tau\phi_2(x)$.
The summation terms on right hand side of (11) can be expressed as

$$\alpha_0 \sum_{l=0}^{n} b_l (u^{n+1-l} - 2u^{n-l} + u^{n-1-l}) + \gamma_1 \tau \alpha_0 \sum_{l=0}^{n} b_l (u^{n+1-l} - u^{n-l}) =$$
$$\alpha_0 (1 + \gamma_1 \tau) \left[u^{n+1} + \sum_{l=0}^{n-1} (b_{l+1} - b_l) u^{n-l} - b_n u^0 \right] + \tag{13}$$
$$\alpha_0 \left[u^n + \sum_{l=0}^{n-1} (b_{l+1} - b_l) u^{n-1-l} - b_n u^1 + 2 b_n \tau \phi_1(x) \right]. \tag{14}$$

The equation (11) can be written as

$$(\alpha_0(1 + \gamma_1 \tau) + \gamma_2) u^{n+1} = \alpha_0 (1 + \gamma_1 \tau) \Big(\sum_{l=0}^{n-1} (b_l - b_{l+1}) u^{n-l} + b_n u^0 \Big) - \alpha_0 u^n +$$
$$\alpha_0 \Big(\sum_{l=0}^{n-1} (b_l - b_{l+1}) u^{n-1-l} + b_n u^1 - 2 b_n \tau \phi_1(x) \Big) + \gamma_3 (u^{n+1})_{xx} + f^{n+1}. \tag{15}$$

Substitute the approximations (8) into (11) for full discretization,

$$
\begin{aligned}
&((\alpha_0+\gamma_1\tau\alpha_0+\gamma_2)a_1-\gamma_3a_4)c_{i-1}^{n+1}+((\alpha_0+\gamma_1\tau\alpha_0+\gamma_2)a_2-\gamma_3a_5)c_i^{n+1}+\\
&((\alpha_0+\gamma_1\tau\alpha_0+\gamma_2)a_1-\gamma_3a_4)c_i^{n+1}=\\
&(2\alpha_0+\gamma_1\tau\alpha_0)(a_1c_{i-1}^n+a_2c_i^n+a_1c_{i+1}^n)-\alpha_0(a_1c_{i-1}^{n-1}+a_2c_i^{n-1}+a_1c_{i+1}^{n-1})\\
&-\gamma_1\alpha_0\tau\sum_{l=1}^{n}b_l\left((a_1c_{i-1}^{n+1-l}+a_2c_i^{n+1-l}+a_1c_{i+1}^{n+1-l})-(a_1c_{i-1}^{n-l}+a_2c_i^{n-l}+a_1c_{i+1}^{n-l})\right)\\
&-\alpha_0\sum_{l=1}^{n}b_l\Big((a_1c_{i-1}^{n+1-l}+a_2c_i^{n+1-l}+a_1c_{i+1}^{n+1-l})-2(a_1c_{i-1}^{n-l}+a_2c_i^{n-l}+a_1c_{i+1}^{n-l})+\\
&(a_1c_{i-1}^{n-1-l}+a_2c_i^{n-1-l}+a_1c_{i+1}^{n-1-l})\Big)+a_1(c_{i+1}^{n+1-l}-2c_{i+1}^{n-l}+c_{i+1}^{n-1-l}))+f_i^{n+1}.
\end{aligned}
\tag{16}
$$

The equation (16) consists of $(M+1)$ linear equations in $M+3$ unknowns. To obtain a unique solution to the system, we need two additional equations which can be obtained by utilizing the given boundary conditions (3). These two additional equations are given by $a_1c_0^n+a_2c_1^n+a_1c_2^n=\psi_1(t)$ and $a_1c_{M-1}^n+a_2c_M^n+a_1c_{M+1}^n=\psi_2(t)$. As a result a diagonal matrix of dimension $(M+3)\times(M+3)$ is obtained which can be solved using any Gaussian elimination based numerical algorithm.

§3 Stability Analysis

This section deals with the stability analysis of the fully discrete scheme (16). By Duhamels' principle [26] it tends to be presumed that the stability analysis for an inhomogeneous problem is an immediate result of the stability analysis for the corresponding homogeneous case. So it is adequate to present the stability analysis for the force free case $f=0$ only. In this study, we assume the growth factor of a Fourier mode to be ω_i^n and let $\tilde{\omega}_i^n$ be its approximation. Define $\Omega_i^n=\omega_i^n-\tilde{\omega}_i^n$ so that from (16), we obtain the following round off error equation

$$
\begin{aligned}
&((\alpha_0+\gamma_1\tau\alpha_0+\gamma_2)a_1-\gamma_3a_4)\Omega_{i-1}^{n+1}+((\alpha_0+\gamma_1\tau\alpha_0+\gamma_2)a_2-\gamma_3a_5)\Omega_i^{n+1}+\\
&((\alpha_0+\gamma_1\tau\alpha_0+\gamma_2)a_1-\gamma_3a_4)\Omega_{i+1}^{n+1}=\\
&(2\alpha_0+\gamma_1\tau\alpha_0)(a_1\Omega_{i-1}^n+a_2\Omega_i^n+a_1\Omega_{i+1}^n)-\alpha_0(a_1\Omega_{i-1}^{n-1}+a_2\Omega_i^{n-1}+a_1\Omega_{i+1}^{n-1})\\
&-\gamma_1\alpha_0\tau\sum_{l=1}^{n}b_l\Big((a_1\Omega_{i-1}^{n+1-l}+a_2\Omega_i^{n+1-l}+a_1\Omega_{i+1}^{n+1-l})-(a_1\Omega_{i-1}^{n-l}+a_2\Omega_i^{n-l}\\
&+a_1\Omega_{i+1}^{n-l})\Big)-\alpha_0\sum_{l=1}^{n}b_l\Big((a_1\Omega_{i-1}^{n+1-l}+a_2\Omega_i^{n+1-l}+a_1\Omega_{i+1}^{n+1-l})-2(a_1\Omega_{i-1}^{n-l}\\
&+a_2\Omega_i^{n-l}+a_1\Omega_{i+1}^{n-l})+(a_1\Omega_{i-1}^{n-1-l}+a_2\Omega_i^{n-1-l}+a_1\Omega_{i+1}^{n-1-l})\Big).
\end{aligned}
\tag{17}
$$

The error equation satisfies the boundary conditions

$$\Omega_0^n=\psi_1(t_n),\quad \Omega_M^n=\psi_2(t_n),\quad n=0,1,\cdots,N, \tag{18}$$

and the initial conditions

$$\Omega_i^0=\phi_1(x_i),\quad (\Omega_t)_i^0=\phi_2(x_i),\quad i=1,2,\cdots,M-1. \tag{19}$$

Define the grid function,

$$\Omega^n(x)=\begin{cases}\Omega_i^n, & x_i-\frac{h}{2}<x\le x_i+\frac{h}{2}\quad i=1,\cdots,M-1\\ 0, & a<x\le\frac{h}{2}\ or\ (b-a)-\frac{h}{2}<x\le(b-a).\end{cases}$$

Note that the Fourier expansion of $\Omega^n(x)$ is

$$\Omega^n(x)=\sum_{m=-\infty}^{\infty}\eta_n(m)e^{\frac{i2\pi mx}{(b-a)}},n=0,1,\cdots,N,$$

where $\eta_n(m)=\frac{1}{(b-a)}\int_a^b\Omega^n(x)e^{\frac{-i2\pi mx}{(b-a)}}dx$. Let

$$\Omega^n=[\Omega_1^n,\Omega_2^n,\cdots,\Omega_{M-1}^n]^T$$

and introduce the norm

$$\|\Omega^n\|_2=\left(\sum_{i=1}^{M-1}h|\Omega_i^n|^2\right)^{\frac{1}{2}}=\left[\int_a^b|\Omega^n(x)|^2dx\right]^{\frac{1}{2}}.$$

By Parseval equality, it is observed that

$$\int_a^b|\Omega^n(x)|^2dx=\sum_{m=-\infty}^{\infty}|\eta_n(m)|^2,$$

so that the following relation is obtained

$$\|\Omega^n\|_2^2=\sum_{m=-\infty}^{\infty}|\eta_n(m)|^2. \tag{20}$$

Suppose that equations (17)-(19) have solution of the form $\Omega_i^n=\eta_n e^{I\theta is}$, where $I=\sqrt{-1}$ and θ is real. Substituting this expression into (17), dividing by $e^{I\theta is}$, using the relation $e^{-I\theta s}+e^{I\theta s}=2cos(\theta s)$ and collecting the like terms, we obtain

$$\begin{aligned}&\Big((\alpha_0+\gamma_1\tau\alpha_0+\gamma_2)a_1-\gamma_3a_4)2\cos(\theta s)+((\alpha_0+\gamma_1\tau\alpha_0+\gamma_2)a_2-\gamma_3a_5)\Big)\eta_{n+1}=\\&\Big((2\alpha_0+\gamma_1\tau\alpha_0)a_12\cos(\theta s)+(2\alpha_0+\gamma_1\tau\alpha_0)a_2\Big)\eta_n-(\alpha_0a_12\cos(\theta s)+\alpha_0a_2)\eta_{n-1}\\&-\gamma_1\alpha_0\tau\sum_{l=1}^n b_l\Big((2a_1\cos(\theta s)+a_2)\eta_{n+1-l}-(2a_1\cos(\theta s)+a_2)\eta_{n-l}\Big)\\&-\alpha_0\sum_{l=1}^n b_l\Big((2a_1\cos(\theta s)+a_2)\eta_{n+1-l}-2(2a_1\cos(\theta s)+a_2)\eta_{n-l}\\&+(2a_1\cos(\theta s)+a_2)\eta_{n-1-l})\Big).\end{aligned} \tag{21}$$

Without loss of generality, we can assume that $\theta=0$, so that (21) reduces to

$$\begin{aligned}&\Big((\alpha_0+\gamma_1\tau\alpha_0+\gamma_2)(2a_1+a_2)-\gamma_3(2a_4+a_5)\Big)\eta_{n+1}=\\&\Big((2\alpha_0+\gamma_1\tau\alpha_0)(2a_1+a_2)\Big)\eta_n-\alpha_0(2a_1+a_2)\eta_{n-1}-\gamma_1\alpha_0\tau\sum_{l=1}^n b_l\end{aligned}$$

$$\Big((2a_1+a_2)(\eta_{n+1-l}-\eta_{n-l}\Big)-\alpha_0(2a_1+a_2)\sum_{l=1}^{n}b_l\Big(\eta_{n+1-l}-2\eta_{n-l}+\eta_{n-1-l})\Big). \tag{22}$$

Hence,

$$\eta_{n+1}=\frac{A_1}{\zeta}\eta_n-\frac{A_2}{\zeta}\eta_{n-1}-\frac{A_3}{\zeta}\sum_{l=1}^{n}b_l(\eta_{n+1-l}-\eta_{n-l})-\frac{A_2}{\zeta}\sum_{l=1}^{n}b_l\Big(\eta_{n+1-l}-2\eta_{n-l}+\eta_{n-1-l}\Big), \tag{23}$$

where,
$\zeta=\Big(1-\frac{\gamma_3}{\alpha_0(1+\gamma_1\tau)+\gamma_2}(\frac{2a_4+a_5}{2a_1+a_2})\Big)$, $A_1=\frac{2\alpha_0+\gamma_1\tau\alpha_0}{\alpha_0+\gamma_1\tau\alpha_0+\gamma_2}$, $A_2=\frac{\alpha_0}{\alpha_0+\gamma_1\tau\alpha_0+\gamma_2}$, $A_3=\frac{\gamma_1\tau\alpha_0}{\alpha_0+\gamma_1\tau\alpha_0+\gamma_2}$.
It is easy to check that $\frac{2a_4+a_5}{2a_1+a_2}=-\frac{3}{4}\tan(\frac{h}{4})^2\leq 0$ so that $\zeta\geq 1$.

Proposition 1. *If η_n $(n=0,1,\cdots N)$ is the solution of equation (23), then $|\eta_n|\leq C|\eta_0|$, where C is the constant given by $C=|A_1|(|A_1|+|A_2|)$.*

Proof. Mathematical induction is used to prove the result. For $n=0$, we have from equation (23) that $\eta_1=\frac{A_1}{\zeta}\eta_0$ and since $\zeta\geq 1$, therefore,

$$|\eta_1|=|\frac{A_1}{\zeta}||\eta_0|\leq|A_1||\eta_0|\leq|A_1|(|A_1|+|A_2|)|\eta_0|=C|\eta_0|.$$

Now suppose that $|\eta_i|\leq|A_1||\eta_0|\leq C|\eta_0|$, $i=1,\cdots,n$ so that from (23), we obtain

$$\begin{aligned}|\eta_{n+1}|\leq{}&\frac{|A_1|}{\zeta}|\eta_n|+\frac{|A_2|}{\zeta}|\eta_{n-1}|+\frac{|A_3|}{\zeta}\sum_{l=1}^{n}b_l\Big(|(|\eta_{n+1-l}|-|\eta_{n-l}|)|\Big)+\\&\frac{|A_2|}{\zeta}\sum_{l=1}^{n}b_l\Big(|(|\eta_{n+1-l}|-2|\eta_{n-l}|+|\eta_{n-1-l}|)|\Big)\\&\leq|A_1||\eta_n|+|A_2||\eta_{n-1}|+|A_3|\sum_{l=1}^{n}b_l\Big(|(|\eta_{n+1-l}|-|\eta_{n-l}|)|\Big)+\\&|A_2|\sum_{l=1}^{n}b_l\Big(|(|\eta_{n+1-l}|-2|\eta_{n-l}|+|\eta_{n-1-l}|)|\Big)\\&\leq|A_1|^2|\eta_0|+|A_1||A_2||\eta_0|+|A_3||A_1|\sum_{l=1}^{n}b_l\Big(|(|\eta_0|-|\eta_0|)|\Big)+\\&|A_2||A_1|\sum_{l=1}^{n}b_l\Big(|(|\eta_0|-2|\eta_0|+|\eta_0|)|\Big)\\&=|A_1|(|A_1|+|A_2|)|\eta_0|=C|\eta_0|,\end{aligned}$$

where, we have used $||a|-|b||\leq|a-b|$. This completes the proof. □

Theorem 1. *The collocation scheme (21) is unconditionally stable.*

Proof. Using formula (20) and Proposition 1, we obtain

$$\|\Omega^n\|_2^2\leq C\|\Omega^0\|_2, n=0,1,\cdots N$$

which establishes unconditional stability. □

§4 Convergence Analysis

In this section, we obtain the following convergence estimates for the time discretized scheme (15).

Theorem 2. *Let $\{u(x,t^n)\}_{n=0}^{N-1}$ be the exact solution of (1) with given initial and boundary conditions and let $\{u^n\}_{n=0}^{N-1}$ be the time discrete solution of (15), then we have the following error estimates*

$$\|e^{n+1}\| \leq E + \Lambda(\tau + \tau^{3-\gamma}),$$

where $e^{n+1} = u(x,t^{n+1}) - u^{n+1}$ and E is a constant.

Proof. It is sufficient to prove the result for $f = 0$. Note that the exact solution u also satisfies the time discretized scheme (15) so that we have

$$\begin{aligned}(\alpha_0(1+\gamma_1\tau)+\gamma_2)u(x,t^{n+1}) = &\\ \alpha_0(1+\gamma_1\tau)\Big(\sum_{l=0}^{n-1}(b_l-b_{l+1})u(x,t^{n-l})+b_n u(x,t^0)\Big)-\alpha_0 u(x,t^n)&\\ +\alpha_0\Big(\sum_{l=0}^{n-1}(b_l-b_{l+1})u(x,t^{n-1-l})+b_n u(x,t^1)-2b_n\tau\phi_1(x)\Big)+\gamma_3(u(x,t^{n+1}))_{xx}&\\ +r_1^{n+1}+r_2^{n+1}.&\end{aligned} \tag{24}$$

Subtracting (15) from (23), we obtain

$$\begin{aligned}&(\alpha_0(1+\gamma_1\tau)+\gamma_2)e^{n+1} =\\ &\alpha_0(1+\gamma_1\tau)\Big(\sum_{l=0}^{n-1}(b_l-b_{l+1})e^{n-l}+b_n e^0\Big)-\alpha_0 e^n+\alpha_0\Big(\sum_{l=0}^{n-1}(b_l-b_{l+1})e^{n-1-l}+b_n e^1\Big)\\ &+\gamma_3(e^{n+1})_{xx}+r_1^{n+1}+r_2^{n+1}.\end{aligned} \tag{25}$$

Using $e^0 = 0$ and taking inner product with e^{n+1} on both sides of (25), we obtain

$$\begin{aligned}&(\alpha_0(1+\gamma_1\tau)+\gamma_2)\|e^{n+1}\|^2 = \alpha_0(1+\gamma_1\tau)\Big(\sum_{l=0}^{n-1}(b_l-b_{l+1})<e^{n-l},e^{n+1}>\Big)-\alpha_0<e^n,e^{n+1}>+\\ &\alpha_0\Big(\sum_{l=0}^{n-1}(b_l-b_{l+1})<e^{n-1-l},e^{n+1}>+b_n<e^1,e^{n+1}>\Big)+\gamma_3<(e^{n+1})_{xx},e^{n+1}>+\\ &<r_1^{n+1},e^{n+1}>+<r_2^{n+1},e^{n+1}>\\ &\leq \alpha_0(1+\gamma_1\tau)\Big(\sum_{l=0}^{n-1}(b_l-b_{l+1})\|e^{n-l}\|\|e^{n+1}\|\Big)-\alpha_0\|e^n\|\|e^{n+1}\|+\\ &\alpha_0\Big(\sum_{l=0}^{n-1}(b_l-b_{l+1})\|e^{n-1-l}\|\|e^{n+1}\|+b_n\|e^1\|\|e^{n+1}\|\Big)-\gamma_3\|(e^{n+1})_x\|^2\\ &+\|r_1^{n+1}\|\|e^{n+1}\|+\|r_2^{n+1}\|\|e^{n+1}\|\\ &\leq \alpha_0(1+\gamma_1\tau)\Big(\sum_{l=0}^{n-1}(b_l-b_{l+1})\|e^{n-l}\|\|e^{n+1}\|\Big)-\alpha_0\|e^n\|\|e^{n+1}\|+\end{aligned}$$

$$\alpha_0\Big(\sum_{l=0}^{n-1}(b_l-b_{l+1})\|e^{n-1-l}\|\|e^{n+1}\|+b_n\|e^1\|\|e^{n+1}\|\Big)+\|r_1^{n+1}\|\|e^{n+1}\|+\|r_2^{n+1}\|\|e^{n+1}\|, \tag{26}$$

where, we have used the relations $< x,x >= \|x\|^2$, $< u_{xx},u >= - < u_x,u_x >= -\|u_x\|^2$, $< x,y >\leq \|x\|\|y\|$ and the fact that $\gamma_3\|(e^{n+1})_x\|^2\geq 0$. Now dividing (26) through out by $\|e^{n+1}\|$, we obtain

$$\begin{aligned}&(\alpha_0(1+\gamma_1\tau)+\gamma_2)\|e^{n+1}\|\\ &\leq \alpha_0(1+\gamma_1\tau)\Big(\sum_{l=0}^{n-1}(b_l-b_{l+1})\|e^{n-l}\|\Big)-\alpha_0\|e^n\|+\alpha_0\Big(\sum_{l=0}^{n-1}(b_l-b_{l+1})\|e^{n-1-l}\|+b_n\|e^1\|\Big)+\\ &\|r_1^{n+1}\|+\|r_2^{n+1}\|\\ &\leq \alpha_0(1+\gamma_1\tau)\Big(\sum_{l=0}^{n-1}(b_l-b_{l+1})\|e^{n-l}\|\Big)+\alpha_0\Big(\sum_{l=0}^{n-1}(b_l-b_{l+1})\|e^{n-1-l}\|+b_n\|e^1\|\Big)+\|r_1^{n+1}\|+\\ &\|r_2^{n+1}\|,\end{aligned} \tag{27}$$

where, we have used the fact that $\alpha_0\|e^n\|\geq 0$. Now let $C_n=\max\limits_{0\leq l\leq n-1}\|e^{n-l}\|$ and $D_n=\max\limits_{0\leq l\leq n-1}\|e^{n-1-l}\|$ so that we obtain from the last inequality

$$\begin{aligned}&(\alpha_0(1+\gamma_1\tau)+\gamma_2)\|e^{n+1}\|\\ &\leq \alpha_0(1+\gamma_1\tau)C_n\sum_{l=0}^{n-1}(b_l-b_{l+1})+\alpha_0D_n\sum_{l=0}^{n-1}(b_l-b_{l+1})+\alpha_0b_n\|e^1\|+\|r_1^{n+1}\|+\|r_2^{n+1}\|\\ &\leq \alpha_0(1+\gamma_1\tau)C_n(1-b_n)+\alpha_0D_n(1-b_n)+\alpha_0b_n\|e^1\|+\|r_1^{n+1}\|+\|r_2^{n+1}\|\\ &\leq \alpha_0(1+\gamma_1\tau)C_n+\alpha_0D_n+\alpha_0\|e^1\|+\|r_1^{n+1}\|+\|r_2^{n+1}\|,\end{aligned} \tag{28}$$

where, we have used $0<b_n<1$. Let $C=\max\limits_{0\leq n\leq N-1}C_n$ and $D=\max\limits_{0\leq n\leq N-1}D_n$ so that we obtain from above inequality

$$\begin{aligned}\|e^{n+1}\|&\leq \frac{\alpha_0(1+\gamma_1\tau)C+\alpha_0D+\alpha_0\|e^1\|}{(\alpha_0(1+\gamma_1\tau)+\gamma_2)}+\frac{\|r_1^{n+1}\|+\|r_2^{n+1}\|}{(\alpha_0(1+\gamma_1\tau)+\gamma_2)},\\ &\leq \frac{\alpha_0(1+\gamma_1\tau)C+\alpha_0D+\alpha_0\|e^1\|}{(\alpha_0(1+\gamma_1\tau)+\gamma_2)}+\Lambda(\tau+\tau^{3-\gamma})=E+\Lambda(\tau+\tau^{3-\gamma}),\end{aligned} \tag{29}$$

where $E=\frac{\alpha_0(1+\gamma_1\tau)C+\alpha_0D+\alpha_0\|e^1\|}{(\alpha_0(1+\gamma_1\tau)+\gamma_2)}$. This completes the proof. □

§5 Numerical experiments and discussion

In this section some numerical experiments are performed to obtain approximate solution of the TFTE(1) with initial (2) and boundary conditions (3). The accuracy of the method is measured through the error norms L_2 and L_∞ and the root means square error (RMSE) given by

$L_2 = \|U^{\text{exact}} - U_N\|_2 \simeq \sqrt{h \sum_{i=1}^{M+1} |U_i^{\text{exact}} - (U_N)_i|}$, $L_\infty = \|U^{\text{exact}} - U_N\|_\infty \simeq \max_i |U_i^{\text{exact}} - (U_N)_i|$ and RMSE $= \sqrt{\frac{\sum_{i=1}^{M}(U_i^{\text{exact}} - (U_N)_i)^2}{M}}$ respectively, where U_i^{exact} is the exact and $(U_N)_i$ is the approximate solution in the spatial domain. The order of converge is calculated by using the formula, Order $= \frac{\log(\frac{\text{Error}(x_i)}{\text{Error}(x_{i+1})})}{\log(\frac{x_i}{x_{i+1}})}$. Numerical results are compared with those of some existing numerical techniques.

Example 1. *Consider the TFTE (1) in* $[0,1]$ *with* $\gamma_1 = 1,\ \gamma_2 = 1$ *and* $\gamma_3 = \pi$ *with initial conditions* $u(x,0) = 0, u_t(x,0) = 0,$ *and the boundary conditions* $u(0,t) = 0, u(1,t) = t^3 \sin^2(1)$.

The exact solution of the problem is $u(x,t) = t^3 \sin^2(x)$ [10, 25, 27] . The corresponding source term $f(x,t)$ is given by $f(x,t) = \frac{6t^{3-\gamma}}{\Gamma(4-\gamma)} \sin^2(x) + \frac{6t^{4-\gamma}}{\Gamma(5-\gamma)} \sin^2(x) + t^3 \sin^2(x) - 2\pi t^3(\cos^2(x) - \sin^2(x))$. In Table 1, the error norms are compared with those of [27] for $\gamma = 1.50,\ \tau = 0.001$ at $t = 1$ for different values of M. Table 2 compares error norms with those obtained in [27] for $\gamma = 1.50, M = 30$ at $t = 1$ for different values of τ. In Table 3, we compute RMSE and compare the results with those of [25]. In Table 4, the approximate solutions for various values of γ are tabulated when $h = \frac{1}{40}, \tau = 0.01, t = 1$. Note that for large values of parameters, the methods of [25, 27] give better accuracy than ours but for small values of parameter our methods performs better. Figure 1 displays the comparison between the exact and approximate solutions at different time levels. The graph shows a tremendous similarity between the solutions. Figure 2 shows 2D and 3D error plots at $t = 0.5$. In Figure 3, a 3D comparison between the exact and approximate solutions is displayed at $t = 1$.

Table 1: Error norms for Example 1 when $\gamma = 1.5,\ \tau = 0.001,\ t = 1$ for different values of M.

M	$L_2 \times 10^3$			$L_\infty \times 10^3$		
	Present method	Galerkin [27]	Order	Present method	Galerkin [27]	Order
5	0.328095	3.798931	1. 691	0.523870	4.929548	1. 791
10	0.101615	0.822230	1. 366	0.151427	1.096321	1. 475
15	0.058402	0.304328	1. 039	0.083268	0.408051	0.815
20	0.043312	0.130208	0.778	0.065857	0.171718	1. 178
25	0.036408	0.053079	0.587	0.050630	0.070520	0.592
30	0.032708	0.020029	-	0.045452	0.033970	-

Table 2: Error norms for Example 1 when $\gamma = 1.5,\ M = 30,\ t = 1$ for different values of τ.

τ	$L_2 \times 10^3$			$L_\infty \times 10^3$		
	Present method	Galerkin [27]	Order	Present method	Galerkin [27]	Order
0.1	2.83061	8.338473	1. 047	4.07858	12.975162	1. 050
0.05	1.36994	4.188691	1. 025	1.96936	6.501840	1. 028
0.01	0.26308	0.781645	0.982	0.37666	1.215807	0.988
0.005	0.13322	0.347984	0.872	0.18989	0.545445	0.888
0.001	0.03271	0.020029	-	0.04545	0.033970	-

Table 3: The RMSE for Example 1 for different values of M and γ when $\tau = 0.0001,\ t = 1$.

M	$\gamma = 1.75$			$\gamma = 1.95$		
	Sinc-Legender (degree=3) [25]	Present method	Order	Sinc-Legender (degree=3) [25]	Present method	Order
5	$9.937e-04$	$2.955e-04$	1. 913	$9.578e-04$	$2.809e-04$	1.905
10	$1.598e-04$	$7.845e-05$	1. 882	$1.538e-04$	$7.501e-05$	1.844
15	$3.707e-05$	$3.658e-05$	1. 815	$3.567e-05$	$3.551e-05$	1.751
20	$1.047e-05$	$2.170e-05$	-	$1.008e-05$	$2.146e-05$	-

Table 4: Approximate solutions for many values of γ when $h = \frac{1}{40}, \tau = 0.01, t = 1$ for Example 1.

x	$\gamma = 1.2$	$\gamma = 1.4$	$\gamma = 1.6$	$\gamma = 1.8$
0.1	0.010038	0.010045	0.010054	0.010067
0.2	0.039610	0.039623	0.039642	0.039669
0.3	0.087538	0.087557	0.087585	0.087627
0.4	0.151908	0.151932	0.151969	0.152025
0.5	0.230152	0.230180	0.230222	0.230293
0.6	0.319145	0.319174	0.319219	0.319299
0.7	0.415330	0.415358	0.415401	0.415483
0.8	0.514863	0.514886	0.514922	0.514995
0.9	0.613763	0.613777	0.613799	0.613846

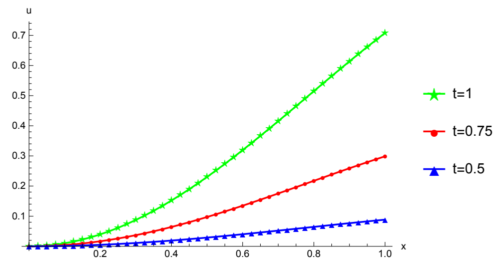

Figure 1: The exact (lines) and approximate (rectangles, stars, bullets) solutions for Example 1 when $M = 80,\ \tau = 0.01$ at different time levels.

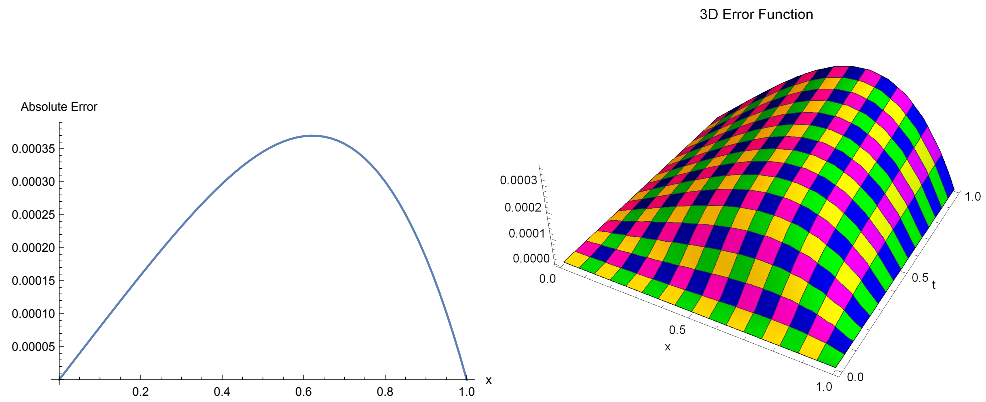

(a) (b)

Figure 2: 2D and 3D absolute error profiles when $M = 60,\ \tau = 0.01,\ t = 1$ for Example 1.

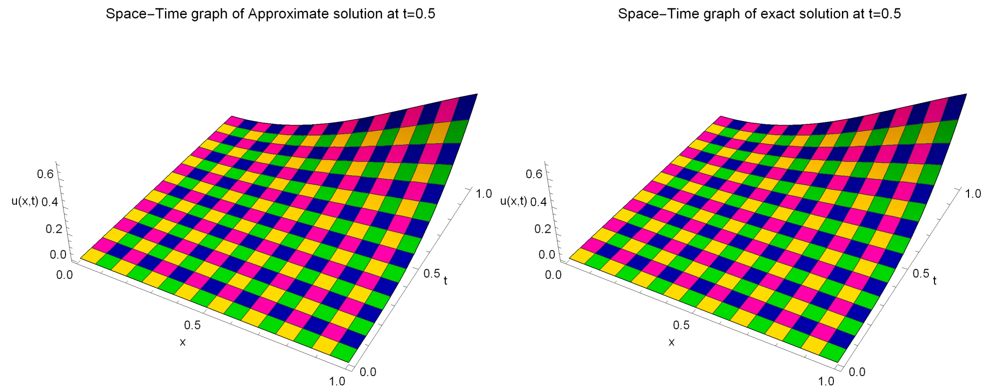

(a) (b)

Figure 3: The exact (right) and numerical (left) solutions when $M = 60,\ \tau = 0.01,\ t = 1$ for Example 1.

Example 2. *Assume* $\gamma_1 = \gamma_2 = \gamma_3 = 1$ *in (1) with initial conditions* $u(x, 0) = x\cos(x^2), u_t(x, 0) = 0$ *and the boundary conditions* $u(0, t) = 0, u(1, t) = \cos(t^2 + 1)$.

The source term $f(x, t)$ is chosen such that the exact solution of the problem is $u(x, t) = x\cos(x^2 + t^2)$ [10]. Table 5 compares the RMSE with those of [10] for different values of γ, M and τ. The comparison reveals that the present method provides better accuracy. In Table 6, the approximate solutions for diverse values of γ are listed by taking $h = \frac{1}{40}, \tau = 0.01, t = 1$. Figure 4 shows a comparison between the exact and approximate solutions at different time levels. An excellent agreement between the solutions can be observed. Figure 5 displays 2D and 3D error plots at time level $t = 1$. An excellent comparison between exact and approximate solutions in 3D is presented in Figure 6 at time step $t = 1$.

Table 5: The RMSE for different values of M, τ and γ for Example 2.

M	τ	$\gamma=1.25$			$\gamma=1.5$			$\gamma=1.75$		
		RBF [10]	Present method	Order	RBF [10]	Present method	Order	RBF [10]	Present method	Order
20	$\frac{1}{10}$	8.620e-03	4.483e-03	1.101	1.038e-02	6.026e-03	1.065	1.217e-02	1.004e-02	1.038
	$\frac{1}{30}$	3.795e-03	1.477e-03	2.303	5.348e-03	1.870e-03	1.109	6.468e-03	3.211e-03	1.138
	$\frac{1}{50}$	2.604e-03	4.555e-04	-	4.099e-03	1.061e-03	-	5.316e-03	1.795e-03	-
50										
	$\frac{1}{10}$	8.772e-03	8.779e-03	1.605	1.056e-02	6.197e-03	1.038	1.239e-02	1.036e-02	1.002
	$\frac{1}{30}$	3.865e-03	1.505e-03	1.011	5.445e-03	1.982e-03	1.138	6.581e-03	3.444e-03	1.055
	$\frac{1}{50}$	2.655e-03	8.981e-04	-	4.174e-03	1.162e-03	-	5.416e-03	2.009e-03	-

Table 6: Approximate solutions for many values of γ when $h=\frac{1}{40}, \tau=0.01, t=1$ for Example 2.

x	$\gamma=1.2$	$\gamma=1.4$	$\gamma=1.6$	$\gamma=1.8$
0.1	0.041992	0.048868	0.057477	0.068599
0.2	0.079641	0.092923	0.109522	0.130923
0.3	0.108299	0.127053	0.150401	0.180375
0.4	0.122781	0.145608	0.173854	0.209847
0.5	0.117256	0.142313	0.173041	0.211746
0.6	0.085366	0.110420	0.140737	0.178305
0.7	0.020650	0.043174	0.069909	0.102284
0.8	-0.082638	-0.065289	-0.045269	-0.021820
0.9	-0.228242	-0.218568	-0.207867	-0.195957

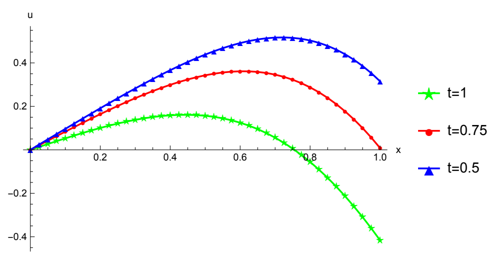

Figure 4: The exact (lines) and approximate (rectangles, stars, bullets) solutions for Example 2 when $M=80,\ \tau=0.01$ at different time levels.

Example 3. *Consider (1) with spatial domain* $[0,1]$ *and* $\gamma_1=\gamma_2=\gamma_3=1$ *with initial conditions* $u(x,0)=0,\quad u_t(x,0)=x(x-1)$ *and the boundary conditions* $u(0,t)=0, u(1,t)=0$.

The exact solution of the problem is $u(x,t)=(x^2-x)t$ [25] so that the corresponding source term is given by $f(x,t)=\left(\frac{\Gamma(2)}{\Gamma(3-\gamma)}t^{2-\gamma}+t\right)(x^2-x)-2t$. In Table 7, absolute errors are computed and the results are compared with those of [25] for $\gamma=1.95$ at $t=1$. The comparison shows better accuracy. In Table 8, the approximate solutions for various values of γ are tabulated using $h=\frac{1}{40}, \tau=0.01, t=1$. In Figure 7, the exact and approximate

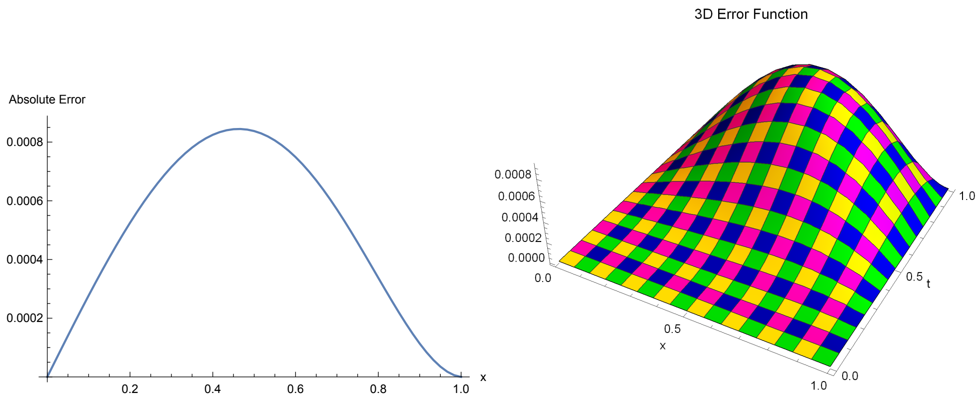

(a) (b)

Figure 5: 2D and 3D absolute error profiles when $M = 60,\ \tau = 0.01,\ t = 1$ for Example 2.

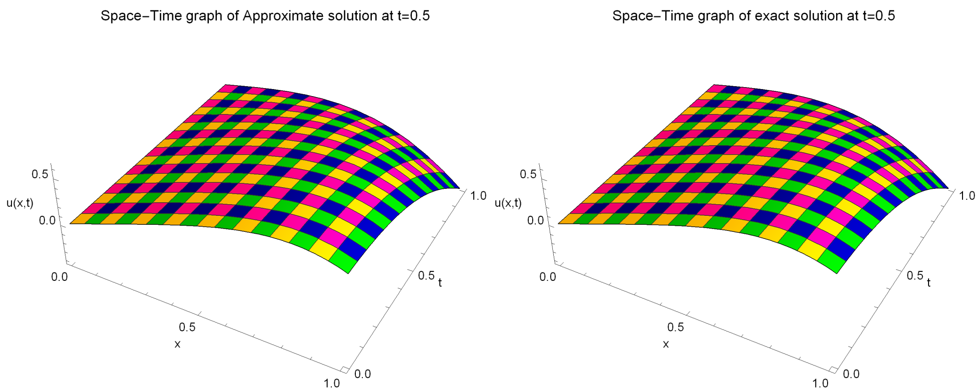

(a) (b)

Figure 6: The exact (right) and numerical (right) solutions when $M = 60,\ \tau = 0.01,\ t = 1$ for Example 2.

solutions are compared at different time levels. Figure 8 displays 2D and 3D error profiles when $M = 60,\ \tau = 0.01$ and $t = 1$. Figure 9 displays a 3D comparison of the exact and approximate solutions when $M = 60,\ \tau = 0.01$ at $t = 1$.

Example 4. *Consider (1) with spatial domain* $[0, 1]$ *and* $\gamma_1 = \gamma_2 = \gamma_3 = 1$ *with initial conditions* $u(x, 0) = 0,\quad u_t(x, 0) = 0$ *and the boundary conditions* $u(0, t) = 0, u(1, t) = t^\gamma \tan(1)$.

The exact solution of the problem is $u(x, t) = t^\gamma \tan x$ so that the corresponding source term is $f(x, t) = \gamma(1 + t) \tan x\Gamma(\gamma) - 2t^\gamma \tan^3 x - t^\gamma \tan x$. In Table 9 different error norms are tabulated for various values of M by taking $\tau = 0.01,\ \gamma = 1.5,\ t = 1$. Table 10 records various error norms for different values of τ when $M = 160, \gamma = 1.5, t = 1$. Figure 10 displays the exact and approximate solutions at different time levels. An close similarity between the solutions can

Table 7: The comparison of absolute errors when $\gamma = 1.95,\ \tau = 0.001$ at $t = 1$ for Example 3.

x	$M = 5$		$M = 7$		$M = 10$	
	Sinc-Legendre [25] (degree=3)	Present method	Sinc-Legendre [25] (degree=3)	Present method	Sinc-Legendre [25] (degree=3)	Present method
0	0	0	0	0	0	0
0.1	1.63e-03	6.40e-04	1.69e-04	3.16e-04	2.90e-04	1.52e-04
0.2	2.48e-03	1.08e-03	1.09e-03	5.51e-04	3.79e-04	2.66e-04
0.3	2.32e-03	1.42e-03	1.07e-03	7.08e-04	3.82e-04	3.45e-04
0.4	2.18e-03	1.59e-03	1.01e-03	8.04e-04	3.64e-04	3.91e-04
0.5	2.15e-03	1.67e-03	9.93e-04	8.38e-04	3.55e-04	4.06e-04
0.6	2.18e-03	1.59e-03	1.01e-03	8.04e-04	3.64e-04	3.91e-04
0.7	2.32e-03	1.42e-03	1.07e-03	7.08e-04	3.82e-04	3.45e-04
0.8	2.47e-03	1.08e-03	1.09e-03	5.51e-04	3.79e-04	2.66e-04
0.9	1.63e-03	6.40e-03	7.69e-04	3.16e-04	2.90e-04	1.52e-04
1	0	0	0	0	0	0

Table 8: Approximate solutions for many values of γ when $h = \frac{1}{40}, \tau = 0.01, t = 1$ for Example 3.

x	$\gamma = 1.2$	$\gamma = 1.4$	$\gamma = 1.6$	$\gamma = 1.8$
0.1	-0.090009	-0.090009	-0.090009	-0.090010
0.2	-0.160016	-0.160016	-0.160016	-0.160017
0.3	-0.210020	-0.210021	-0.210021	-0.210021
0.4	-0.240023	-0.240023	-0.240024	-0.240024
0.5	-0.250024	-0.250024	-0.250025	-0.250025
0.6	-0.240023	-0.240023	-0.240024	-0.240024
0.7	-0.210020	-0.210021	-0.210021	-0.210021
0.8	-0.160016	-0.160016	-0.160016	-0.160017
0.9	-0.090009	-0.090009	-0.090009	-0.090010

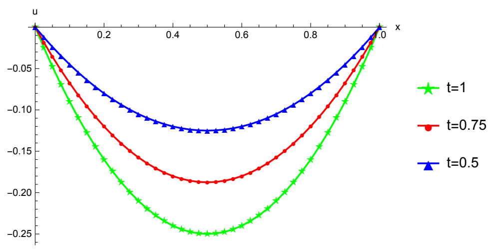

Figure 7: The exact (lines) and approximate (rectangles, stars, bullets) solutions for Example 4 when $M = 80,\ \tau = 0.01$ at different time levels.

be seen. Figure 11 displays 2D and 3D error plots at time level $t = 1$. An excellent comparison between exact and approximate solutions in 3D is presented in Figure 12 at time step $t = 1$.

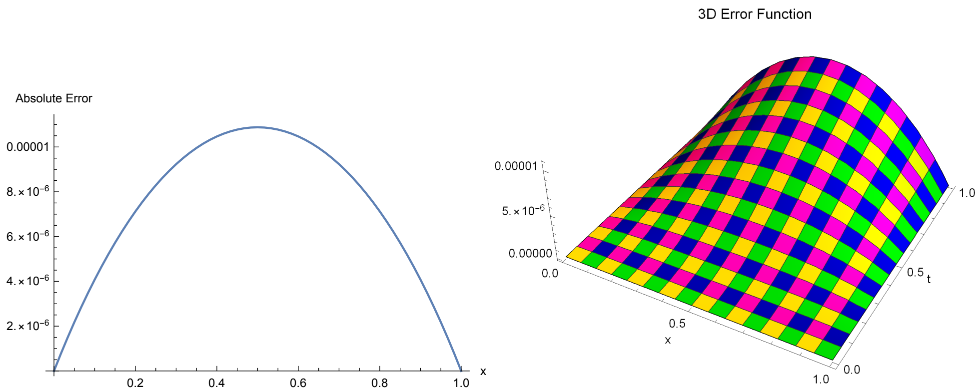

(a) (b)

Figure 8: 2D and 3D absolute error profiles when $M = 60,\ \tau = 0.01,\ t = 1$ for Example 3.

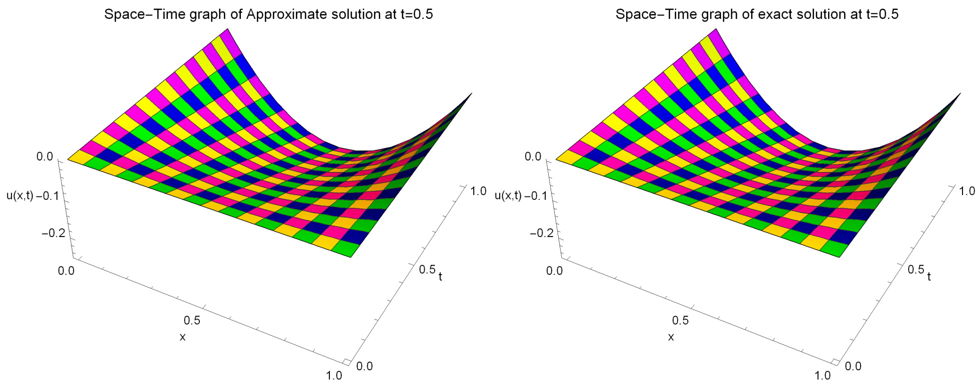

(a) (b)

Figure 9: The exact (right)and numerical (left) solutions when $M = 60,\ \tau = 0.01,\ t = 1$ for Example 3.

Table 9: The error norms for different values of M when $\tau = 0.01,\ \gamma = 1.5,\ t = 1$ for Example 4.

M	Absolute Error	L_2- Error	RMS Error
20	2.8836×10^{-3}	2.0593×10^{-3}	2.010×10^{-3}
40	2.2937×10^{-3}	1.6414×10^{-3}	1.6212×10^{-3}
80	2.1497×10^{-3}	1.5381×10^{-3}	1.5285×10^{-3}
160	2.1141×10^{-3}	1.5123×10^{-3}	1.5076×10^{-3}

Table 10: The error norms for different values of τ when $M = 40,\ \gamma = 1.5,\ t = 1$ for Example 4.

τ	Absolute Error	L_2- Error	RMS Error
0.0125	2.5626×10^{-3}	1.8344×10^{-3}	1.8119×10^{-3}
0.01	2.2936×10^{-3}	1.6414×10^{-3}	1.6212×10^{-3}
0.00125	9.1459×10^{-4}	6.5344×10^{-4}	6.4542×10^{-4}
0.001	2.1497×10^{-3}	1.5381×10^{-3}	1.5285×10^{-3}

Table 11: Approximate solutions for many values of γ when $h = \frac{1}{40}, \tau = 0.01, t = 1$ for Example 4.

x	$\gamma = 1.2$	$\gamma = 1.4$	$\gamma = 1.6$	$\gamma = 1.8$
0.1	0.097472	0.099345	0.100106	0.100388
0.2	0.197123	0.200778	0.202255	0.202782
0.3	0.301305	0.306556	0.308663	0.309374
0.4	0.412752	0.419314	0.421919	0.422752
0.5	0.534860	0.542334	0.545264	0.546164
0.6	0.672102	0.679959	0.682995	0.683912
0.7	0.830711	0.838267	0.841139	0.842010
0.8	1.019870	1.026250	1.028630	1.029360
0.9	1.253960	1.258020	1.259490	1.259950

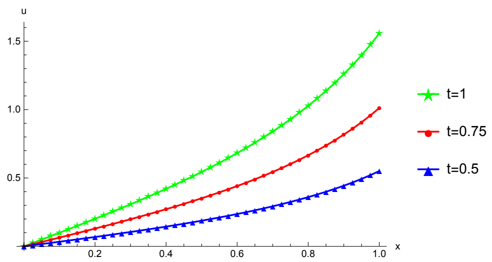

Figure 10: The exact (lines) and approximate (rectangles, stars, bullets) solutions for Example 4 when $M = 80,\ \tau = 0.01$ at different time levels.

§6 Concluding Remarks

This investigation exhibits a numerical procedure dependent on cubic trigonometric B-spline for the TFTE. The scheme utilized the usual finite difference scheme to approximate the Caputo time-fractional derivative and the derivative in space are approximated using the cubic trigonometric B-spline basis functions. Exceptional consideration has been given to examine the stability and convergence analysis of the scheme. The obtained outcomes are contrasted with those of some current procedures. The comparison uncovers that the presented scheme is comparable with other existing techniques for TFTE regarding precision, adaptability, and proficiency. In addition, the scheme can be applied to a large class of fractional order partial differential equations with some modifications.

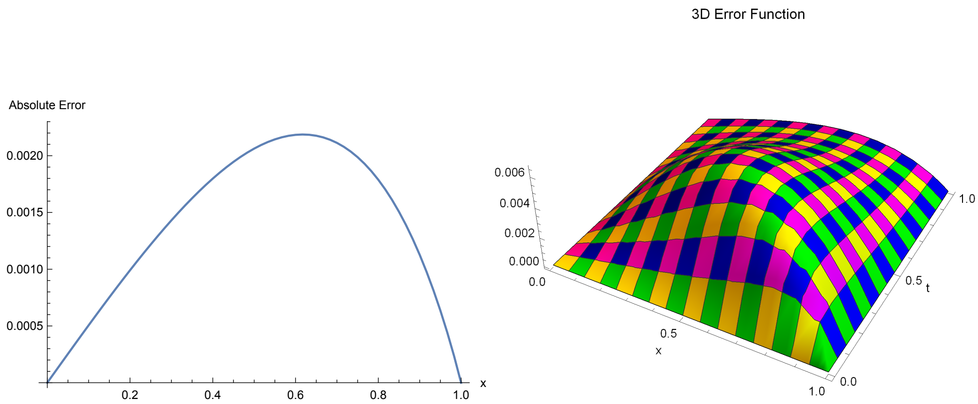

Figure 11: 2D and 3D absolute error profiles when $M = 60,\ \tau = 0.01,\ t = 1$ for Example 4.

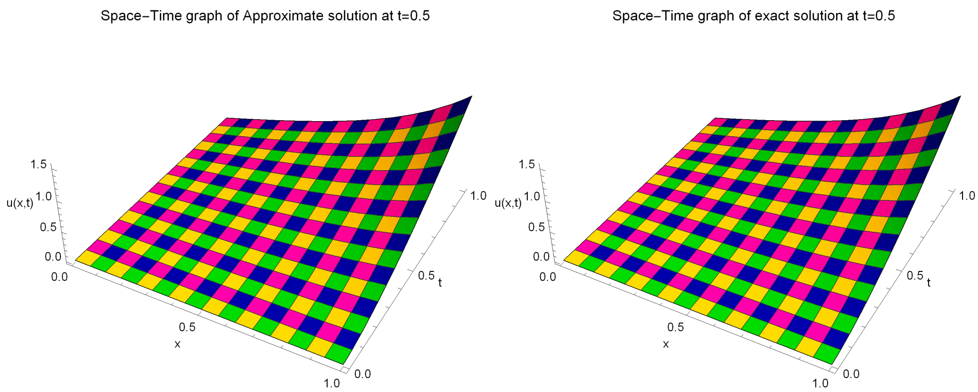

Figure 12: The exact (right) and numerical (right) solutions when $M = 60,\ \tau = 0.01,\ t = 1$ for Example 4.

References

[1] M Abbas, A A Majid, A I M Ismail, A Rashid. *The application of cubic trigonometric B-spline to the numerical solution of the hyperbolic problems*, Appl Math Comput, 2014, 239: 74-88.

[2] T Akram , M Abbas, A I Ismail, N H M Ali, D Baleanu. *Extended cubic B-splines in the numerical solution of time fractional telegraph equation*, Adv Differ Equ, 2019, 365: 1-20.

[3] M Amin, M Abbas, M K Iqbal, D Baleanu. *Non-polynomial quintic spline for numerical solution of fourth-order time fractional partial differential equations*, Adv Differ Equ, 2019, 183: 1-22.

[4] M Amin, M Abbas, M K Iqbal, A I Ismail, D Baleanu. *A fourth order non-polynomial quintic spline collocation technique for solving time fractional superdiffusion equations*, Adv Differ Equ, 2019, 514: 1-21.

[5] J Banasiak, J R Mika. *Singularly perturbed telegraph equations with appplications in the random walk theory*, J Appl Math Stoch Anal, 1998, 11(1): 9-28.

[6] C de Boor. *A Practical Guide to Splines*, 1978, Springer-Verlag.

[7] J Chen, F Liu, V Anh. *Analytical solution for the time-fractional telegraph equation by the method of separating variables*, J Math Anal Appl, 2008, 338(2): 1364-1377.

[8] W Hachbusch. *Integral equations theory and numerical treatments*, 1995:120, Birkhäuser Basel.

[9] M S Hashemi, D Baleanu. *Numerical approximation of higher-order time-fractional telegraph equation by using a combination of a geometric approach and method of line*, J Comput Phys, 2016, 316: 10-20.

[10] V R Hosseini, W Chen, Z Avazzadeh. *Numerical solution of fractional telegraph equation by using radial basis functions* , Eng Anal Bound Elem, 2014, 38: 31-39.

[11] G Hariharan, R Rajaraman, M Mahalakshmi. *Wavelet method for a class of space and time fractional telegraph equations*, Int J Phys Sci, 2012, 7 (10): 1591-1598.

[12] R Hilfer. *Applications of fractional calculus in physics*, 2000, World Scientific, Singapore.

[13] W Jiang, Y Z Lin. *Representation of exact solution for the time-fractional telegraph equation in the reproducing kernel space*, Commun Nonlinear Sci Numer Simul, 2011, 16: 3639-3645.

[14] P Jordan, A Puri. *Digital signal propagation in dispersive media*, J Appl Phys, 1999, 85(3): 1273-1282.

[15] N Khalid, M Abbas, M K Iqbal. *Non-polynomial quintic spline for numerical solution of fourth-order Time Fractional Partial Differential Equations*, Appl Math and Comput, 2019, 349: 393-401.

[16] N Khalid, M Abbas, M K Iqbal, D Baleanu. *A numerical algorithm based on modified extended B-spline functions for solving time-fractional diffusion wave equation involving reaction and damping terms*, Adv Differ Equ, 2019, 378: 1-19

[17] A A Kilbas, H M Srivastava, J J Trujillo. *Theory and applications of fractional differential equations*, 2006, Elsevier Science BV, Amsterdam.

[18] S Kumar. *A new analytical modeling for fractional telegraph equation via Laplace transform*, Appl Math Model, 2014, 38: 3154-3163.

[19] S T Mohyud-Din, T Akram, M Abbas, A I Ismail, N H M Ali. *A fully implicit finite difference scheme based on extended cubic B-splines for time fractional advection–diffusion equation*, Adv Differ Equ, 2018, 109: 1-17.

[20] S Momani. *Anaalytic and approximate solutions of the space- and time-fractional telegraph equations*, Appl Math Comput, 2005, 176: 1126-1134.

[21] N Mollahasani, M M Moghadam, K Afrooz. *A new treatment based on hybrid functions to the solution of telegraph equations of fractional orfer*, Appl Math Model, 2016, 40 (4), 2804-2814.

[22] E Orsinger, X Zhao. *The space-fractional telegraph equation and the related fractional telegraph process*, Chin Ann Math, 2004, 24: 45-56.

[23] I Podlubny. *Fractional differential equations*, 1999, Academic Press.

[24] P M Prenter. *Splines and variational methods*, 1989, John Wiley and Sons.

[25] N H Sweilam, A M Nagy, A A Al-Sayed. *Solving time-fractional order telegraph equation via Sinc-Legendre collocation ethod*, Mediterr J Math, 2016, 13: 5119-5133.

[26] J C Strikwerda. *Fninite diffrence schemes and partial diffrential equations*, 2^{nd} edition, 2004, SIAM.

[27] O Tasbozan, A Esen. *Quadratic B-spline Galerkin method for numerical solution of fractional telegraph equations*, J Math Sci Appl, 2017, 18: 23-29.

[28] V A Vyawahare, P Nataraja. *Fractional order modelling of neurtron transport in a nuclear reactor*, Appl Math Model, 2013, 37(23): 9747-9767.

[29] L L Wei, H Dai, D L Zhang, Z Y Si. *Fully discrete local discontinuous Galerkin method for solving the fractional telegraph equaiton*, Calcolo., 2014, 51: 175-192.

[30] Y L Wang, M J Du, C L Temuer, D Tian. *Using reproducing kernel for solving a class of time-fractional telegraph equation with initial value conditions*, Int J Comput Math, 2017: 1-13.

[31] M Yaseen, M Abbas, A I Ismail, T Nazir. *A cubic trigonometric B-spline collocation approach for the fractional sub-diffusion equations*, Appl Math Comput, 2017, 293: 311-319.

[32] M Yaseen, M Abbas, T Nazir, D Baleanu. *A finite difference scheme based on cubic trigonometric B-splines for time fractional diffusion-wave equation*, Adv Differ Equ, 2017, 274: 1-18.

[33] M Yaseen, M Abbas. *An efficient computational technique based on cubic trigonometric B-splines for time fractional Burgers' equation*, International journal of Computer Mathematics, 2020, 97 (3): 725-738.

[34] A Yildirim. *He's homtopy perturbation method for solving the space and time fractional telegraph equations*, Int J Comput Math, 2010, 87 (13): 2998-3006.

Department of Mathematics, University of Sargodha, Sargodha 40100, Pakistan.
Email: yaseen.yaqoob@uos.edu.pk , muhammad.abbas@uos.edu.pk